Manuscript submitted Oct. 5, 1993; revised manuscript received Jan. 18, 1994.

The University of Connecticut assisted in meeting the publication costs of this article.

REFERENCES

1. P. Tatapudi and J. M. Fenton, in *Electrochemical Engineering and Small Scale Electrolytic Processing,* C. W. Walton, R. D. Varjian, and J. W. Van Zee, Editors, PV 90-10, p. 275, The Electrochemical Society Proceedings Series, Pennington, NJ (1990).
2. P. Tatapudi and J. M. Fenton, *This Journal,* **140,** 3527 (1993).
3. P. Tatapudi and J. M. Fenton, *ibid.,* **140,** L55 (1993).
4. P. C. Foller and C. W. Tobias, *ibid.,* **129,** 506 (1982).
5. J. A. McIntyre and R. F. Phillips, in *Electrochemical Process and Plant Design,* R. C. Alkire, T. R. Beck, and R. D. Varjian, Editors, PV 83-6, p. 79, The Electrochemical Society Proceedings Series, Pennington, NJ (1983).
6. E. E. Kalu and C. Oloman, *J. Appl. Electrochem.,* **20,** 932 (1990).
7. K. Otsuka and I. Yamanaka, *Electrochim. Acta,* **35,** 319 (1990).
8. G. Bianchi, F. Mazza, and T. Mussini, *ibid.,* **2,** 1509 (1966).
9. S. Stucki, G. Theis, R. Kotz, H. Devantay, and H. J. Christen, *This Journal,* **132,** 367 (1985).
10. S. Stucki, H. Baumann, H. J. Christen, and R. Kotz, *J. Appl. Electrochem.,* **17,** 773 (1987).
11. P. Tatapudi, Ph.D. Thesis, University of Connecticut, Storrs, CT (1993).
12. J. A. Appleby and E. B. Yeager, in *Assessment of Research Needs for Advanced Fuel Cells,* prepared by S. S. Penner for U.S. Dept. of Energy under Contract No. DE-AC01-84ER30060, pp. 137-152 (1985).

An Investigation of Spinel-Related and Orthorhombic $LiMnO_2$ Cathodes for Rechargeable Lithium Batteries

R. J. Gummow and M. M. Thackeray*,[a]

Division of Materials Science and Technology, CSIR, Pretoria 0001, South Africa

ABSTRACT

Cathode materials that have been synthesized by reduction of lithium-manganese-oxide and manganese-oxide precursors with hydrogen at 300 to 350°C, and with carbon at 600°C have been evaluated in rechargeable lithium cells. The cathodes which initially have a composition close to $LiMnO_2$ contain structures related to the lithiated-spinel phase $Li_2[Mn_2]O_4$ and/or orthorhombic $LiMnO_2$. The orthorhombic $LiMnO_2$ component transforms gradually to a spinel structure on cycling. These cathodes are significantly more tolerant to repeated lithium insertion and extraction, when cycled over both the 4 and 3 V regions, than a standard $Li_x[Mn_2]O_4$ spinel electrode ($0 < x < 2$).

"Rocking-chair" cells, with intercalation electrodes as both cathode and anode, are being developed for commercial rechargeable lithium battery applications. Because these cells do not contain metallic lithium, they are far safer than conventional lithium cells. On the first charge cycle, lithium ions are extracted from the cathode and inserted into the anode; cathode materials which can be prepared chemically in the discharged state, such as $LiCo_yNi_{1-y}O_2$ ($0 \leq y \leq 1$) and $Li[Mn_2]O_4$ are therefore required for this type of cell.[1-6]

Carbon is an attractive anode material that can be used as a host for accommodating lithium in rocking-chair cells; it provides high capacity, good reversibility, and a low voltage (<1 V) *vs.* lithium over a wide compositional range Li_xC_6 ($0 \leq x \leq 1$).[3,6] Some lithium is, however, always irreversibly consumed by a carbon anode on the first charge cycle. To compensate for the lithium that is not released from the anode (which can account for at least 20% of the anode capacity), an excess of discharged cathode is initially required when cells are assembled. This has the disadvantage of reducing the overall energy density of the cell. Alternatively, additional lithium may be incorporated within the cathode structure to yield an "over-discharged" state which is possible, for example, with a $Li_x[Mn_2]O_4$ spinel cathode.[7] $Li_x[Mn_2]O_4$ operates at approximately 4 V *vs.* lithium over the range $0 < x \leq 1$ and has a theoretical capacity of 154 mAh/g based on the mass of the fully oxidized electrode (MnO_2). In practice, a rechargeable cathode capacity of approximately 120 to 130 mAh/g can be achieved from $Li_x[Mn_2]O_4$ cathodes at moderate current rates.[6,8] $Li_x[Mn_2]O_4$ is therefore, in principle, an attractive cathode for $C/Li_x[Mn_2]O_4$ rocking-chair cells. Moreover, surplus lithium can be introduced into the $Li_x[Mn_2]O_4$ structure over the range $1 \leq x \leq 2$ to balance the capacity loss at the carbon anode on the first cycle. Unfortunately, the maximum benefit of the surplus capacity in the $Li_x[Mn_2]O_4$ cathode cannot be fully utilized in a rocking-chair cell, first, because the $Li_x[Mn_2]O_4$ electrode operates at a significantly reduced voltage over the compositional range $1 \leq x \leq 2$ and, second, because the $Li_x[Mn_2]O_4$ electrode is structurally unstable over this range which leads to a rapid loss of electrode capacity on cycling.

Tarascon *et al.*[7] have demonstrated the use of LiI as a lithiating agent for the preparation of $Li_{1+x}[Mn_2]O_4$ spinel electrodes. Although this technique can be carried out in air, it is expensive to apply on an industrial scale. A simple and cheap processing route for synthesizing lithium-manganese-oxide cathodes with an excess lithium capacity is therefore required. $Li_{1+x}[Mn_2]O_4$ materials cannot be synthesized directly in air because of the tendency of the manganese ions to oxidize and to form compounds in the $Li_2O \cdot yMnO_2$ system, for example, the rock salt phase Li_2MnO_3 ($y = 1$) and the $Li_2O \cdot yMnO_2$ spinels ($2.5 \leq y \leq 4.0$). In this paper we describe alternative methods for the chemical synthesis of lithium cathodes in the "over-discharged" state with structures characteristic of spinel-related and orthorhombic $LiMnO_2$ materials, and we examine their electrochemical properties in room temperature lithium cells.

Experimental

Attempts were made to synthesize cathodes with stoichiometry $LiMnO_2$ from various precursors according to the ideal reactions given below. The reactions were carried out with a reducing agent to lower the valency of the manganese ions, either with hydrogen or with carbon in the

* Electrochemical Society Active Member.
[a] Present address: Chemical Technology Division, Argonne National Laboratory, Argonne, IL 60439.

presence of an inert gas, at temperatures between 300 and 600°C

$$LiMn_2O_4 + LiOH \cdot H_2O + 0.5H_2 \xrightarrow{300 \text{ to } 400\ ^\circ C} 2LiMnO_2 + 2H_2O \quad [1]$$

$$2Li_4Mn_5O_{12} + 2Li_2MnO_3 + 3C \xrightarrow[Ar]{600^\circ C} 12LiMnO_2 + 3CO_2 \quad [2]$$

$$2MnO_2(\gamma) + 2LiOH \cdot H_2O + C \xrightarrow[Ar]{600^\circ C} 2LiMnO_2 + CO_2 + 2H_2O \quad [3]$$

Reaction 1.—The $Li[Mn_2]O_4$ precursor was prepared by the reaction of Li_2CO_3 and $MnCO_3$, in a 1:4 molar ratio. The mixture was initially ball-milled in hexane for 24 h and thereafter heated in air at 850°C for 48 h. The reaction with $LiOH \cdot H_2O$ was carried out under a constant flow of dry hydrogen gas at 300°C for 20 h (sample A), 350°C for 3 h (sample B) and at 400°C for 20 h (sample C).

Reaction 2.—A precursor consisting of a two-phase, intergrown structure of $Li_4Mn_5O_{12}$ and Li_2MnO_3 was synthesized by the reaction of Li_2CO_3 and $MnCO_3$ in a 1:2 molar ratio in air at 400°C for 48 h. (Note that this precursor has an overall composition "$Li_2Mn_2O_5$" in which the Li:Mn ratio is 1:1). Acetylene black [25 mole percent (m/o)] was added to the precursor and the mixture reacted in a tube furnace under a constant flow of dry argon at 600°C for 20 h (sample D).

Reaction 3.—γ-MnO_2 (EMD) was intimately mixed with $LiOH \cdot H_2O$ (Li:Mn = 1:1) and acetylene black (25 m/o) in a ballmill and thereafter heated at 600°C for 2 h under argon. The product was cooled slowly to room temperature in the furnace (sample E).

Two standard $LiMnO_2$ compounds were synthesized according to previously reported methods. A lithiated spinel $Li_2[Mn_2]O_4$ was prepared by the reaction of $Li[Mn_2]O_4$ with an excess of LiI under reflux in acetonitrile in air at 82°C for several hours.[7] The product was washed with acetonitrile to remove any excess LiI and dried in air at 80°C. Orthorhombic-$LiMn_2O_2$ was synthesized by the reaction of γ-MnO_2 (CMD), $LiOH \cdot H_2O$, and acetylene black at 620°C under argon for 20 h.[9]

Powder x-ray diffraction patterns of the samples were obtained from an automated Rigaku powder diffractometer with CuKα radiation that was monochromated by a graphite single crystal. Lattice parameters were refined against an internal silicon standard.

The cathode materials were mixed with acetylene black and ethylene propylene diene monomer (EPDM) binder and cycled against lithium anodes in flooded electrolyte cells. A full description of the cell construction is given elsewhere.[10] Cellgard microporous membranes were used to separate the electrodes; the electrolyte was a 1*M* solution of $LiClO_4$ in propylene carbonate. Cells were charged and discharged at current rates that varied from 0.05 to 0.2 mA/cm^2 between voltage limits that ranged from 4.4 V at the top of charge to 2.0 V at the end of discharge.

Results and Discussion

The powder x-ray diffraction patterns of the $Li[Mn_2]O_4$, "$Li_2Mn_2O_5$," and γ-MnO_2 precursors that were used to synthesize the $LiMnO_2$ cathode materials are shown in Fig. 1a-c. The pattern of "$Li_2Mn_2O_5$" (Fig. 1b) is characteristic of an intergrowth structure of a $Li_4Mn_5O_{12}$ spinel phase and a Li_2MnO_3 rocksalt phase, the individual x-ray diffraction patterns of which are remarkably similar. The indexed powder x-ray diffraction patterns of the two standard, well-known $LiMnO_2$ compounds, namely, the lithiated spinel $Li_2[Mn_2]O_4$ ($F4_1/ddm$) and orthorhombic-$LiMnO_2$ (Pmmn) are depicted in Fig. 2a and b, respectively.

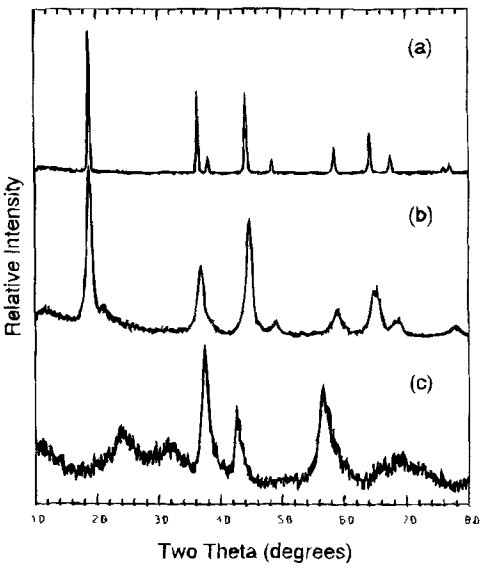

Fig. 1. Powder x-ray diffraction patterns of (a) $Li[Mn_2]O_4$, (b) "$Li_2Mn_2O_5$," and (c) γ-MnO_2 (CMD) precursor materials.

Reaction 1: Reduction of $LiMn_2O_4$ under hydrogen.—Reaction of $Li[Mn_2]O_4$ with $LiOH \cdot H_2O$ under hydrogen results in products that consist essentially of a lithiated-spinel phase, $Li_{1+x}[Mn_2]O_4$ ($x \approx 1$), and a rock salt phase, MnO (Fig. 3a, b); the exact composition of the lithiated-spinel phase in the reaction mixture was difficult to determine. The amount of MnO in the final product is highly dependent on the reaction temperature and time. For example, sample A (300°C, 20 h) (Fig. 3a) and sample B (350°C, 3 h) (Fig. 3b) contain approximately the same relative amounts of the lithiated-spinel phase and MnO, whereas after prolonged reaction at 400°C the pattern is dominated by MnO peaks (Fig. 3c). The *a* lattice parameter of the MnO phase was calculated to be 4.434 (3) Å, which is in good agreement with the literature value for MnO, 4.445 Å.[11] When taken to completion, the reaction under hydrogen can therefore be represented as a two-stage process

$$Li[Mn_2]O_4 + LiOH \cdot H_2O + 0.5H_2 \rightarrow Li_2[Mn_2]O_4 + 2H_2O$$

$$Li_2[Mn_2]O_4 + H_2 \rightarrow 2MnO + 2LiOH$$

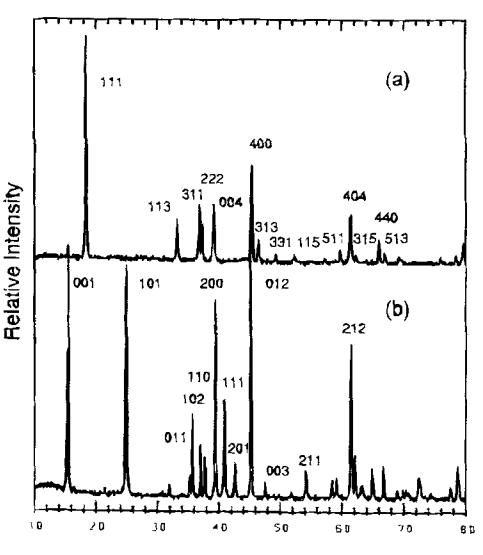

Fig. 2. Powder x-ray diffraction patterns of (a) $Li_2[Mn_2]O_4$ indexed to a face-centered tetragonal unit cell ($F41/ddm$) and (b) $LiMnO_2$ indexed to a primitive orthorhombic unit cell (Pmmn).

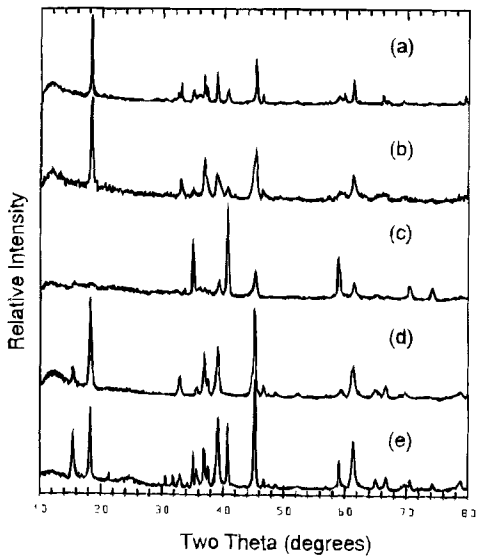

Fig. 3. Powder x-ray diffraction patterns of (a) sample A, (b) sample B, (c) sample C, (d) sample D, and (e) sample E.

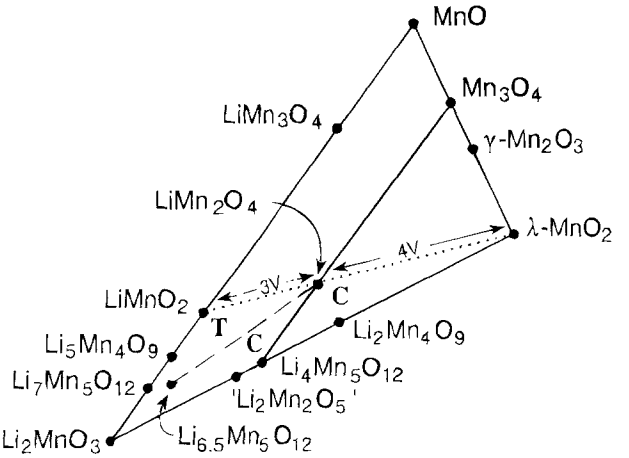

Fig. 4. An isothermal slice of a section of the ternary Li-Mn-O phase diagram.

In practice, it is not easy to control the formation of a single-phase $Li_2[Mn_2]O_4$ product under hydrogen. It is particularly difficult to prevent the formation of MnO on the surface of the lithiated-spinel particles which could be detrimental to the electrochemical activity of the spinel electrode, because MnO is electrochemically inactive. "$LiMnO_2$" compounds synthesized under hydrogen are unstable; they decompose if exposed to air.

This study therefore demonstrates, in particular, that under appropriate reducing conditions, a tetragonal lithiated spinel can be synthesized from simple precursors. This contrasts with the attempts of Barboux *et al.* to synthesize tetragonal $Li_2[Mn_2]O_4$ from manganese acetate and lithium acetate by annealing the reagents at 400°C at low oxygen pressures in argon;[12] they reported that the products were always multiphase mixtures that contained $Li[Mn_2]O_4$ and either MnO or Li_2MnO_3.

It is of interest to note that the extent of the Jahn-Teller distortion in the lithiated-spinel phases in samples A and B is not as pronounced as it is in the $Li_2[Mn_2]O_4$ product made from LiI (Table I). The smaller *c* lattice parameters and *c/a* values are indicative of lithiated-spinel phases that lie on the tie-line between $LiMnO_2$ (alternatively, $Li_2[Mn_2]O_4$) and $Li_7Mn_5O_{12}$ (alternatively, $Li_2[Mn_{1.67}Li_{0.33}]O_4$) in the Li-Mn-O phase diagram (Fig. 4). This diagram relates specifically to the compositions of (*i*) stoichiometric-spinel phases, (*ii*) defect-spinel phases, and (*iii*) lithiated-spinel phases with a rock salt stoichiometry. The weakening of the Jahn-Teller effect in the lithiated-spinel phases as the rock salt composition changes from $Li_2[Mn_2]O_4$ (c/a = 1.158, c = 9.274 Å, a = 8.006 Å) through $Li_5Mn_4O_9$ (c/a = 1.142, c = 9.150 Å, a = 8.011 Å)[13] to $Li_7Mn_5O_{12}$ (c/a = 1.108, c = 8.906 Å, a = 8.036 Å)[13] is clearly a result of the decrease in Mn^{3+} concentration; in $Li_2[Mn_2]O_4$, $Li_5Mn_4O_9$, and $Li_7Mn_5O_{12}$ the average Mn oxidation state increases from 3.00 to 3.25 and 3.40, respectively. The values of the *c* parameters of the lithiated spinel phases in samples A and B (9.259 and 9.232 Å, respectively) indicate, therefore, that the composition of these phases deviates slightly from $Li_2[Mn_2]O_4$ (c = 9.274 Å) and that the oxidation state of the manganese ions is marginally greater than 3.0.

Table I. Lattice parameters of lithiated-spinel products.

Sample	a (Å)	c (Å)	c/a
Sample A	8.004(2)	9.259(4)	1.157(1)
Sample B	8.011(11)	9.232(35)	1.152(6)
Sample D	8.038(4)	9.218(8)	1.147(2)
Sample E	8.029(5)	9.187(9)	1.144(2)
$Li_2[Mn_2]O_4$	8.006(2)	9.274(4)	1.158(1)
$Li_5Mn_4O_9$ [13]	8.011(-)	9.150(-)	1.142(-)
$Li_7Mn_5O_{12}$ [13]	8.036(-)	8.906(-)	1.108(-)

Reactions 2 and 3: Reduction of precursors with carbon.—Carbon is a significantly milder reducing agent than hydrogen and consequently higher temperatures were employed to reduce the "$Li_2Mn_2O_5$" and γ-MnO_2 precursors. An advantage of this technique is that any carbon that remains in the sample after the reaction will enhance the electronic conductivity of the electrode. Moreover, because carbon is a mild reducing agent, it is easier to limit the amount of MnO by-product. The powder x-ray diffraction patterns of the products of reactions are shown in Fig. 3d (sample D) and Fig. 3e (sample E). Both samples contain a lithiated-spinel component and an orthorhombic-$LiMnO_2$ component. Sample D consists predominantly of the lithiated-spinel phase, whereas in Sample E there is more orthorhombic-$LiMnO_2$, which is evident from the more intense characteristic peak at ~15.6° 2θ, some MnO, and some unreacted LiOH · H_2O. A longer reaction time at 600°C ensures that the reaction goes to completion; in this case a single-phase orthorhombic $LiMnO_2$ is produced at the expense of the lithiated-spinel phase (Fig. 2b).[9] The values of the *c* lattice parameters of the lithiated-spinel phases in samples D (c = 9.218 Å) and *E* (c = 9.187 Å) are indicative of structures that contain less Mn^{3+} than those in samples A and B (Table I) and have compositions closer to $Li_5Mn_4O_9$ (c = 9.150 Å); this finding is not surprising, considering that mild reducing conditions were used and that the manganese ions in the initial "$Li_2Mn_2O_5$" and γ-MnO_2 precursors were tetravalent.

Electrochemical characterization.—It has recently been established that orthorhombic $LiMnO_2$ electrodes are electrochemically active when synthesized at moderate temperature[14] and, when cycled in lithium cells, transform to a spinel-related structure.[9] It is also well-known that the $[B_2]X_4$ framework of an $A[B_2]X_4$ spinel can provide a stable host structure for lithium.[13,14] The electrochemical data that follows is therefore interpreted in terms of lithium insertion and extraction reactions that occur with spinel-type structures. Spinel and defect-spinel electrodes of principle interest in the Li-Mn-O system are found within the MnO_2-$Li[Mn_2]O_4$-$Li_4Mn_5O_{12}$ tie-triangle of the phase diagram (Fig. 4); they all have cubic symmetry, Fd3m. These electrodes deliver capacity at ~4 and at ~3 V against lithium depending on the composition of the spinel. The 4 V electrode is obtained, in general, when lithium is inserted into, or extracted from, the tetrahedral A sites, whereas a 3 V electrode is obtained when lithium is inserted into, or extracted from, the interstitial and B octahedral sites of the spinel structure. Lithium insertion/extraction reactions follow the dotted lines in Fig. 4, for example, between λ-MnO_2 ($[Mn_2]O_4$) and $LiMnO_2$ ($Li_2[Mn_2]O_4$), and

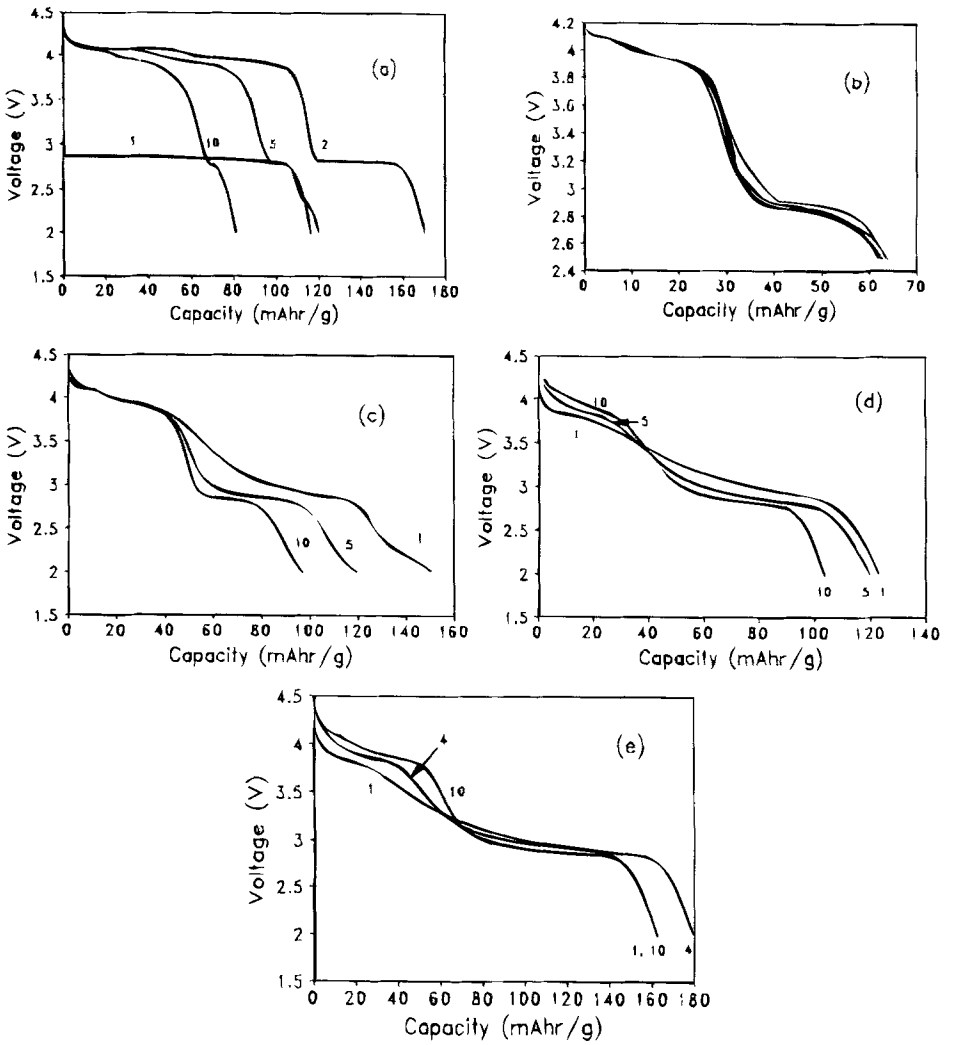

Fig. 5. Galvanostatic discharge curves of (a) a standard Li/$Li_x[Mn_2]O_4$ cell (0.1 mA/cm^2, (b-e) Li/"$LiMnO_2$" cells: (b) sample A (0.2 mA/cm^2), (c) sample B (0.1 mA/cm^2), (d) sample D (0.1 mA/cm^2), and (e) sample E (0.1 mA/cm^2).

between $Li_4Mn_5O_{12}$ ($Li[Mn_{1.67}Li_{0.33}]O_4$) and $Li_7Mn_5O_{12}$ ($Li_2[Mn_{1.67}Li_{0.33}]O_4$).

$Li/Li_x[Mn_2]O_4$ cells have been characterized in detail;[6,8] for $0 < x \leq 1$, lithium is inserted into the tetrahedral sites at ~4 V in a two-stage process which is attributed to an ordering of the lithium ions on half of the tetrahedral sites (8a) of the spinel structure at $x \approx 0.5$. The two-stage process is indicated by a small voltage step (~100 mV) during discharge and charge. At $x \approx 1.08$, a cooperative displacement of the tetrahedral-site lithium ions into neighboring interstitial octahedral sites generates a two-phase electrode (at ~3 V) that consists of $Li_{1.08}[Mn_2]O_4$ and a lithiated-spinel phase $Li_2[Mn_2]O_4$ with a rock salt stoichiometry.[15]

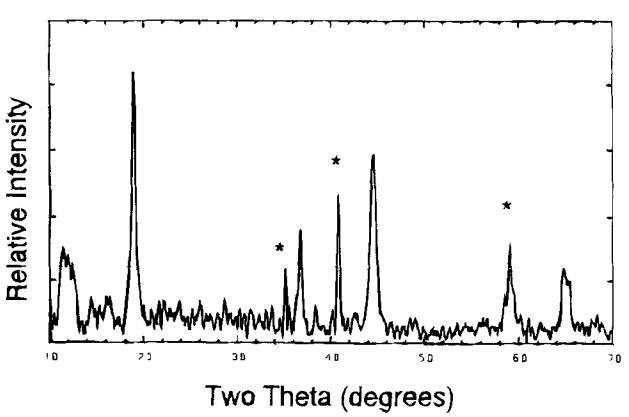

Fig. 6. Powder x-ray diffraction pattern of a partially discharged sample E cathode after 10 cycles. MnO peaks are indicated with an asterisk.

Lithium insertion reactions into lithium-manganese-oxide spinel structures induce a Jahn-Teller distortion when the average manganese oxidation state reaches approximately 3.5.[13] Spinel electrodes that initially have a composition between λ-MnO_2 and $Li_4Mn_5O_{12}$ in Fig. 4 therefore maintain their cubic symmetry until the composition of the electrode reaches the tie-line between $LiMn_2O_4$ and $Li_{6.5}Mn_5O_{12}$ which is a line of constant manganese valence (3.5). For example, in the 3 V region of the phase diagram, a cubic $Li_{1+x}[Mn_2]O_4$ electrode distorts to tetragonal symmetry almost immediately ($x \approx 0.08$), whereas a $Li_{4+x}Mn_5O_{12}$ electrode retains its cubic symmetry deep into discharge until the composition reaches $Li_{6.5}Mn_5O_{12}$ ($x = 2.5$). The Jahn-Teller effect is deleterious for rechargeable lithium cells; the asymmetric change in unit cell parameters which is reflected by a significant change in the c/a ratio and which can vary from 10 to 16% (Table I), destroys the structural integrity of the spinel electrode on cycling. Spinel electrodes should therefore ideally be cycled in the cubic region of the Li-Mn-O phase diagram in which compositional variations are accompanied by an isotropic expansion/contraction of the unit cell. $Li_{4+x}Mn_5O_{12}$ is therefore a significantly more stable 3 V electrode than $Li_{1+x}Mn_2O_4$.[13] $Li_xMn_2O_4$ can operate at both 4 and 3 V; on the other hand, $Li_4Mn_5O_{12}$ ($Li[Mn_{1.67}Li_{0.33}]O_4$) operates only as a 3 V electrode because lithium cannot be extracted from the tetrahedral sites as the Mn ions are all tetravalent.

Characterization of a standard $Li_x[Mn_2]O_4$ electrode.—A $Li/Li_x[Mn_2]O_4$ cell was used as a standard cell against which the performance of the samples A, B, D, and E could be evaluated. This cell, which was assembled with a stan-

dard $LiMn_2O_4$ cathode, was discharged and charged over both the 3 and 4 V plateaus. The voltage profiles of the 1st, 2nd, 5th, and 10th cycles are given in Fig. 5a. The data are in good agreement with previous studies of this system.[16] Capacity is lost rapidly on the 3 V plateau because of the Jahn-Teller effect and an associated degradation of the spinel structure. Consequently, the electrode capacity at 4 V is reduced significantly on cycling.

Characterization of samples A, B, D, and E.—The electrochemical discharge characteristics of samples A, B, D, and E are given in Fig. 5b-d. All cells were subjected to an initial charge. The capacity delivered on the subsequent discharge was 65-80% of the initial capacity drawn from the cell; this initial capacity loss is believed to be associated with damage to the cathode structures during the transformation of the tetragonal lithiated-spinel phase to a cubic structure and during the transition of the orthorhombic-$LiMnO_2$ phase to a spinel-type structure.

Samples A and B (produced by reduction with H_2 at 300 and 350°C).—The discharge performance of cells with samples A and B that contained initially a lithiated-spinel phase and some MnO are shown in Fig. 5b and c, respectively. Sample A shows a voltage profile typical of a spinel electrode with the characteristic two-step process at 4 V and a plateau at 3 V (Fig. 5b). The total capacity delivered by the electrode is, however, only 62 mAh/g. The low capacity was attributed partly to a low concentration of electronic conductor (acetylene black) that was added to this particular cathode, and also to the possibility that MnO on the surface of the lithiated spinel particles may have restricted the diffusion of the lithium ions in and out of the spinel structure. Despite the low capacity delivered, the cycling efficiency was remarkably stable on both the 4 V plateau (~30 mAh/g) and 3 V plateau (~30 mAh/g). This performance strongly suggests that the cubic symmetry of the spinel host structure is maintained throughout charge and discharge, and that insufficient lithium could be inserted into the electrode to induce the transformation to tetragonal symmetry.

Although a significantly higher capacity was delivered by sample B [it provided 130 mAh/g to 2.5 V on the first discharge (Fig. 5c)], capacity was lost steadily on the 3 V plateau during successive cycles, indicating that this electrode, like the standard $Li_x[Mn_2]O_4$ electrode (Fig. 5a) was discharged substantially into the tetragonal region of the phase diagram. However, unlike the $Li_x[Mn_2]O_4$ electrode, surprisingly little capacity was delivered at 4 V (45 mAh/g); this capacity was retained on cycling.

Samples D and E (produced by reduction with carbon at 600°C).—The discharge profiles of cells containing samples D and E, both of which initially contained a lithiated-spinel component and an orthorhombic-$LiMnO_2$ component, are shown in Fig. 5d and e, respectively. Although the discharge is essentially spinel-like in character, the discharge profiles change on cycling, with the capacity at 4 V increasing at the expense of the capacity at 3 V. This phenomenon is consistent with the trend shown during the electrochemical transformation of orthorhombic $LiMnO_2$ to a spinel-related structure; it is associated with the occupation of an increasing number of tetrahedral sites as the $[Mn_{2-y}Li_y]O_4$ ($0 \leq y \leq 0.33$) spinel framework develops in the electrode.[9] The phenomenon is also consistent with the fact that for spinel-related structures, for example $Li_x[Mn_2]O_4$, the 4 V plateau is more stable to cycling than the 3 V plateau, the former being associated with a cubic electrode structure ($0 < x \leq 1$), whereas the latter is associated with a two-phase (cubic and tetragonal) electrode ($1 \leq x \leq 2$). The powder x-ray diffraction pattern of sample E, partially discharged, after 10 cycles, is shown in Fig. 6. The dominant broader peaks are characteristic of a cubic spinel structure. The sharp peaks are characteristic of electrochemically inactive MnO; they are also present in the pattern of the original electrode structure (Fig. 3e). Of particular significance is the high rechargeable capacity delivered by sample E (derived from a γ-MnO_2 precursor). Although the cell suffered a gradual capacity loss on cycling, the electrode still delivered 160 mAh/g after 10 cycles, 60 mAh/g of which was associated with the 4 V plateau and 100 mAh/g with the 3 V plateau. Such a performance could be anticipated from a spinel electrode with nominal composition $Li_2Mn_5O_{11}$ (or alternatively, $Li_2O \cdot 5MnO_2$) which, from the Li-Mn-O phase diagram would be expected to deliver with respect to $Li_{2+x}Mn_5O_{11}$, 72 mAh/g at 4 V ($0 \leq x \leq 1.25$), 72 mAh/g in the 3 V cubic region ($1.25 \leq x \leq 2.50$) and 87 mAh/g in the 3 V tetragonal region ($2.50 \leq x \leq 4.00$). In $Li_{2+x}Mn_5O_{11}$, 45% of the discharge at 3 V is associated with a cubic structure which could account for the relatively slow drop in capacity at 3 V compared with the standard $Li_x[Mn_2]O_4$ electrode. Furthermore, the lattice parameters of a tetragonal rocksalt-phase $Li_6Mn_5O_{11}$, that is located between $Li_5Mn_4O_9$ and $LiMnO_2$ on the Li-Mn-O phase diagram, would be expected to be close to the values determined for sample E (Table I).

Conclusions

The possibility of synthesizing electrodes with an approximate composition $LiMnO_2$ for rechargeable lithium batteries has been investigated by reducing lithium-manganese-oxide and manganese-oxide precursors with hydrogen and with carbon. The best electrochemical data were obtained when carbon was used as the reducing agent, from electrodes that were initially comprised of an intergrown lithiated-spinel and orthorhombic-$LiMnO_2$ structure, but which transformed on cycling to a single-phase spinel compound.

Spinel electrodes that can accommodate lithium within a cubic structure at 3 V (*vs.* lithium) are significantly more stable than $Li_x[Mn_2]O_4$ to cycling between 4.4 and 2 V when the electrode is allowed to vary over a wide compositional range. Structural stability and capacity retention of the spinel electrode at 3 V are, however, gained at the expense of capacity at 4 V, which limits the utility of these electrodes for rocking-chair cells with carbon anodes.

Manuscript submitted Nov. 9, 1993; revised manuscript received Jan. 23, 1994.

CSIR assisted in meeting the publication costs of this article.

REFERENCES

1. E. Plichta, M. Salomon, S. Slane, M. Uchiyama, D. Chua, W. B. Ebner, and H. W. Lin, *J. Power Sources,* **21,** 25 (1987).
2. E. Plichta, S. Slane, M. Uchiyama, M. Salomon, D. Chua, W. B. Ebner, and H. W. Lin, *This Journal,* **136,** 1865 (1989).
3. J. R. Dahn, U. von Sacken, M. W. Juzkow, and H. Al-Janaby, *ibid.,* **138,** 2207 (1991).
4. T. Ohzuku, H. Komori, K. Sawai, and T. Hirai, *Chem. Express,* **5,** 773 (1990).
5. C. Delmas and I. Saadoune, *Solid State Ionics,* **53-56,** 370 (1992).
6. D. Guyomard and J. M. Tarascon, *This Journal,* **139,** 937 (1992).
7. J. M. Tarascon and D. Guyomard, *ibid.,* **138,** 2864 (1991).
8. V. Manev, A. Momchilov, A. Nassalevska, and A. Kozawa, *J. Power Sources,* **43-44,** 551 (1993).
9. R. J. Gummow, D. C. Liles, and M. M. Thackeray, *Mater. Res. Bull.,* In press (1993).
10. R. J. Gummow, Ph.D. Thesis, University of Cape Town, Cape Town, South Africa (1993).
11. JCPDS Powder Diffraction File, 7-230 (1989).
12. P. Barboux, J. M. Tarascon, and F. K. Shokoohi, *J. Solid State Chem.,* **94,** 185 (1991).
13. M. M. Thackeray, A. de Kock, M. H. Rossouw, D. Liles, R. Bittihn, and D. Hoge, *This Journal,* **139,** 364 (1992).
14. T. Ohzuku, A. Ueda, and T. Hirai, *Chem. Express,* **7,** 193 (1992).
15. M. M. Thackeray, W. I. F. David, P. G. Bruce, and J. B. Goodenough, *Mater. Res. Bull.,* **18,** 461 (1983).
16. J. M. Tarascon, E. Wang, F. K. Shokoohi, W. R. McKinnon, and S. Colson, *This Journal,* **138,** 2859 (1991).